

## E. OTHER NUCLEAR STRUCTURE RESEARCH

The return of Gammasphere to ATLAS allows the rich program of gamma-ray spectroscopy to be explored. A variety of programs are being pursued, including studying hot nuclei and nuclei at the very highest angular momenta.

- e.1.  $^{12}\text{C} + ^{12}\text{C}$  Radiative Capture Studies** (D. G. Jenkins, C. J. Lister, M. P. Carpenter, R. V. F. Janssens, T. L. Khoo, T. Lauritsen, N. J. Hammond, R. Wadsworth,<sup>‡</sup> P. Chowdhury,<sup>†</sup> B. R. Fulton,<sup>‡</sup> J. Pearson,<sup>‡</sup> A. H. Wuosmaa,<sup>§</sup> P. Fallon,<sup>¶</sup> A. O. Macchiavelli,<sup>¶</sup> M. McMahan,<sup>¶</sup> A. G3rgen,<sup>¶</sup> and F. Haas<sup>||</sup>)

Radiative capture of light ions, the complete fusion of nuclei without particle emission, is a key mechanism for nucleosynthesis. In astrophysics, the fusion of heavier ions is suppressed, as the high mutual Coulomb barrier between ions demands extraordinary temperatures for reactions to proceed. However, the radiative capture of heavy ions has always had reaction-mechanism and structural interest that has centered around the issue of forming nuclear molecules and their subsequent relaxation into a fused system.

The classic case study for radiative capture is  $^{12}\text{C} + ^{12}\text{C}$ . Here, the scattering and fusion cross-sections are known to have strong, resonant, energy dependence. Many years ago, Sandorfi and Nathan<sup>1,2,3</sup> showed this resonant pattern also persisted in the radiative capture channel, directly connecting the  $^{12}\text{C} + ^{12}\text{C}$  resonant states to the fused  $^{24}\text{Mg}$  groundstate through a single high energy gamma-ray. This key observation opened many issues, one of which concerns the overall magnitude of the radiative fusion cross-section. It is far from clear that single-step decay is favored, and if not,

how much flux passes through intermediate doorway states and how many doorways are involved?

We conducted experiments with Gammasphere and with the FMA in order to address this issue. The Gammasphere experiment was unusual as it exploited the device as a total energy calorimeter to isolate the radiative capture channel that has a uniquely high photon endpoint. Although difficult to calibrate exactly, the total radiative capture appeared to be more than five times stronger than the single step decays reported by Sandorfi and Nathan, and showed strong energy dependence. Most of the decay flux seemed to pass through relatively few intermediate states near 10-MeV excitation in  $^{24}\text{Mg}$ . The FMA experiment, directly counting residues, led to a similar conclusion about the total radiative capture cross-section.

We have finalized analysis of these results and are comparing them to numerical simulation. A Rapid Communication is being prepared.<sup>4</sup> We are planning to conduct similar studies using the DRAGON spectrometer at the ISAC facility at TRIUMF in order to study resonances at lower energy.

<sup>†</sup>University of Massachusetts-Lowell, <sup>‡</sup>University of York, United Kingdom, <sup>§</sup>University of Western Michigan, <sup>¶</sup>Lawrence Berkeley National Laboratory, <sup>||</sup>CNRS-IN2P3, Strasborg, France.

<sup>1</sup>A. M. Sandorfi, *Tretise on Heavy Ion Science*, Vol. 2, Sec. III, ed. D. A. Bromley (Plenum Press, New York 1985).

<sup>2</sup>A. M. Sandorfi and A. M. Nathan, *Phys. Rev. Lett.* **40**, 1252 (1978).

<sup>3</sup>A. M. Nathan, A. M. Sandorfi, and T. J. Bowles, *Phys. Rev. C* **24**, 932 (1981).

<sup>4</sup>D. G. Jenkins *et al.*, to be published in PRL 2004.

**e.2. Shape Evolution in the Superdeformed  $A \sim 80 - 90$  Mass Region** (R. V. F. Janssens, K. Lagergren,<sup>\*1</sup> B. Cederwall,<sup>\*</sup> R. M. Clark,<sup>†</sup> P. Fallon,<sup>†</sup> A. G3rgen,<sup>†</sup> T. Issa,<sup>\*</sup> A. Johnson,<sup>\*</sup> A. O. Macchiavelli,<sup>†</sup> L. Milechina,<sup>\*</sup> D. G. Sarantites,<sup>‡</sup> and R. Wyss<sup>\*</sup>)

Superdeformed bands in  $^{88}\text{Mo}$ ,  $^{89}\text{Tc}$ , and  $^{91}\text{Tc}$  were populated using a  $^{40}\text{Ca}$  beam with an energy of 185 MeV, impinging on a backed  $^{58}\text{Ni}$  target. Gamma rays and charged particles emitted in the reactions were detected using the Gammasphere Ge detector array and the CsI(Tl) array Microball. Average transition quadrupole moments  $Q_t$  were deduced for the bands using the residual Doppler shift technique. The experimental results were included into a systematic

study of the  $Q_t$  values throughout the superdeformed mass 80 – 90 region (see Fig. I-30). The superdeformed shell gaps are predicted to move towards larger deformations with increasing  $Z$  and  $N$  in this mass region. This trend is confirmed by the experimental  $Q_t$  values.

A paper reporting these results was recently published.<sup>1</sup>

<sup>\*</sup>Royal Institute of Technology, Stockholm, Sweden, <sup>†</sup>Lawrence Berkeley National Laboratory, <sup>‡</sup>Washington University.

<sup>1</sup>K. Lagergren *et al.*, Phys. Rev. C **68**, 064309 (2003).

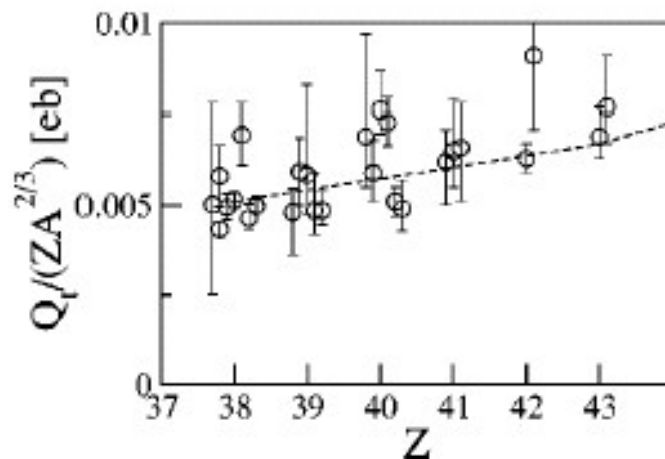


Fig. I-30. Experimentally deduced transition quadrupole moments divided by  $Z^{2/3}$  as a function of  $Z$  for the SD bands in the neutron deficient  $A \sim 80 - 90$  mass region are shown with error bars. The dashed line shows the quadrupole moment as calculated.

### e.3. Rotational Damping, Ridges and the Quasicontinuum of $\gamma$ Rays in $^{152}\text{Dy}$

(T. Lauritsen, I. Ahmad, M. P. Carpenter, A. M. Heinz, R. V. F. Janssens, D. G. Jenkins, T. L. Khoo, F. G. Kondev, C. J. Lister, D. Seweryniak, P. Fallon,\* A. O. Macchiavelli,\* D. Ward,\* R. M. Clark,\* M. Cromaz,\* A. Larabee,§ B. Herskind,† T. Døssing,† A. Lopez-Martens,‡ A. Korichi,‡ and S. Siem‡)

Superdeformation in  $^{152}\text{Dy}$  was originally discovered by studying ridges, i.e. structures along the diagonal, in  $\gamma$ - $\gamma$  matrices.<sup>1</sup> Only afterwards was the first discrete superdeformed (SD) band discovered.<sup>2</sup> It took us 16 years to link the first SD to the normal deformed states it decays into<sup>3</sup> and we also recently linked the SD band,<sup>6</sup> which is built on an octupole vibration, to the yrast SD band.<sup>4</sup> These two feats were only possible because we collected a very large dataset with Gammasphere using the reaction  $^{108}\text{Pd}(^{48}\text{Ca},4n)^{152}\text{Dy}$  at 194 MeV.

This very large dataset allow us to now go back and look at the continuum  $\gamma$  rays with much more precision. Figure I-31 shows the ridges in coincidence with SD band 1 in  $^{152}\text{Dy}$ . Two clean discrete SD  $\gamma$  rays were required before the  $\gamma$ - $\gamma$  matrix is updated. The matrix is then unfolded,<sup>5</sup> corrected for detector efficiency and finally 'core' subtracted.<sup>10</sup> Both the normal (ND) and SD discrete transitions as well as their coincidences along the axis (stripes) are removed (to improve the ridge signal) and a region from 800 keV to 1200 keV is projected normal to the diagonal. The effect of removing the stripes is corrected for. The final result, presented in Fig. I-31, shows a spectacular ridge structure - at least four ridges can easily be seen, as well as a shallow valley and a wide component. Figure I-32 shows the same thing when two clean ND  $\gamma$  rays are required before any updates of the  $\gamma$ - $\gamma$  matrix. Using the procedures outlined in Ref. 6, we also extracted the quasicontinuum (QC) of  $\gamma$  rays in coincidence with SD band 1, Fig. I-33, as well as the QC in coincidence with clean ND lines, Fig. I-34.

The ridges seen in Fig. I-31 and Fig. I-32 stems from correlations of the E2  $\gamma$  rays emitted while the nucleus is hot, i.e. at finite temperature. In this region, where the SD bands are embedded in a sea of hot normal states, a residual interaction will give rise to what is known as rotational damping or broadening of the ridges. There is much interest in measuring this interaction. Recent theoretical calculations show that there is not just one, but two components to this damping.<sup>7</sup>

A simple 'toy model' indicates that there is no way to reproduce the ridges in Fig. I-31 with just one damping width; two components are present, as suggested by

theory. It is also clear that even with two components of damping, it is not possible to reproduce the ridges and the valley at the same time in a simple 'toy model'. Thus, dynamic effects, as taken into account in the Monte Carlo (MC) code `kl_sd/kla`,<sup>6</sup> are important. In this MC code cascades are started from an entry distribution, the area populated in the spin-energy plane after the last particle has been evaporated, and followed through the SD and ND wells in a nucleus until they are close to either the SD or ND yrast lines in the nucleus. Eight decays are considered: three E1 transition with  $\Delta I = -1, 0, +1$  and stretched E2 transitions. The decays are governed by the these eight decays widths, four of which will always be on the 'other side' of the barrier between the SD and ND well and subsequently attenuated by the tunneling probability through the barrier (depending on the excitation energy). This MC code has been very successful in describing the SD  $A = 190$  region.<sup>6</sup>

Using this code, after two rotational damping components were incorporated into it, it is now possible to make a reasonable (yet preliminary) SIMULTANEOUS reproduction (1) the SD ridges (Fig. I-31), (I-32) the ND ridges (Fig. I-32), (I-33) the ND QC (Fig. I-33), and (I-34) the SD QC (Fig. I-34). The latter QC has two components, the upper part from the feeding of SD band 1, the other from the decay of the SD band. As opposed to the  $A = 190$  region, the decay out component is not all that distinct from the feeding component, so, unlike in the  $A = 190$  region, is not so easy to find the excitation energy of a SD band using the QC method described in Ref. 6. Another lesson learned is that the sharp features in the ND ridges in Fig. I-32 are from E2 transitions that happen in the SD well (i.e. SD ridges). The MC calculations indicates that about 1/4 of the quasicontinuum collective E2  $\gamma$  rays in the feeding of the ND states in the nucleus are emitted while the nucleus is superdeformed in this reaction. Thus, the 'ND' ridges in Fig. I-32 are a complex mix of four components: a wide and narrow component in both the ND and SD wells.

In Fig. I-33 and Fig. I-34, in red, are the calculated QC components from the MC code. Even though preliminary, the reproductions are encouraging and confirm the validity of the theory used in the code. It is

very demanding to reproduce so many experimentally extracted spectra with one model and one consistent set of parameters. The code does not yet calculate the  $\gamma$  rays from the last step into the ND and SD yrast lines, which eventually will fill in the missing intensity at the low energies in Figs. I-33 and I-34.

Currently the entry distribution used in the MC code is from the *evapOR* code<sup>8</sup> which does not reproduce the population of the nuclei in the reaction region all that well. We will soon remedy that by a dedicated experiment to MEASURE the entry distribution using Gammasphere as a calorimeter. The SD feeding is preferentially from the low energy, high spin part of the entry distribution. Thus, knowing the entry distribution experimentally, should help the calculation of the ridges and QCs which are sensitive to how this distribution looks like. Also, as Table I-2 indicates, one has to use

different rotational widths in the spin regions relevant to feeding and decay, at high and low spins, respectively. As a matter of fact, there may be wide changes in the rotational damping width as a function of spin and excitation energy  $U^*$ .<sup>9</sup> Indeed, a first attempt to include the spin and excitation energy dependence of the rotational damping is able to reproduce the QC in Fig. I-33 between 2 and 3 MeV much better. Work is in progress on including the variation in spin and excitation energy of  $\Gamma_{\text{rot}}$  properly.

Figure I-35 shows 200  $\gamma$  cascades from the entry distribution to near the ND yrast line. Both E1 and E2 transitions in the ND and SD wells are color-coded. Notice how, at the highest spins, many E2  $\gamma$  rays are emitted in the SD well near the region where the SD band becomes yrast w.r.t. the normal states and where the SD quadrupole strength comes is large.

Table I-2. Parameters used to reproduce the Ridges and QC of  $\gamma$  rays in the feeding region (spins above  $\sim 35 \hbar$ ) and decay region near  $\sim 25 \hbar$ . These are preliminary results.

	<u>ND</u>	<u>SD</u>
$\Gamma_{\text{Rot narrow}}$ [keV] HWHM	28	5
$\Gamma_{\text{Rot wide}}$ [keV] HWHM	305 <sup>a</sup>	170
narrow comp. fraction	0.17	0.30
level dens. par, a	21.7	21.7
Qt[efm <sup>2</sup> ]	700	900
$J^{(1)}$ [ $\hbar^2/\text{MeV}$ ]	73	87

<sup>a</sup>In the decay out region,  $\Gamma_{\text{Rot wide}}$  must be reduced to  $\sim 150$  keV to fit the spectra (see text).

\*Lawrence Berkeley National Laboratory, †Niels Bohr Institute, Copenhagen, Denmark, ‡CSNSM, IN2P3-CNRS, Orsay, France, §Greenville College.

<sup>1</sup>B. Nyako *et al.*, Phys. Rev. Lett. **52**, 507 (1984).

<sup>2</sup>P. J. Twin *et al.*, Phys. Rev. Lett. **55**, 1380 (1985).

<sup>3</sup>T. Lauritsen *et al.*, Phys. Rev. Lett. **88**, 042501 (2002).

<sup>4</sup>T. Lauritsen *et al.*, Phys. Rev. Lett. **89**, 282501 (2002).

<sup>5</sup>D. C. Radford *et al.*, Nucl. Instrum. Methods **A258**, 111 (1987).

<sup>6</sup>T. Lauritsen *et al.*, Phys. Rev. C **62**, 044316 (2000).

<sup>7</sup>M. Matsuo, T. Døssing, B. Herskind, S. Leoni, E. Vigezzi, and R. A. Broglia, Phys. Lett. **B465**, 1 (1999).

<sup>8</sup>by N. G. Nicolis, Wu, and J. R. Beene, ORNL, from ftp.ornl.gov.

<sup>9</sup>B. Lauritzen *et al.*, Nucl. Phys. **A457**, 61 (1986).

<sup>10</sup>O. Andersen *et al.*, Phys. Rev. Lett. **43**, 687 (1979).

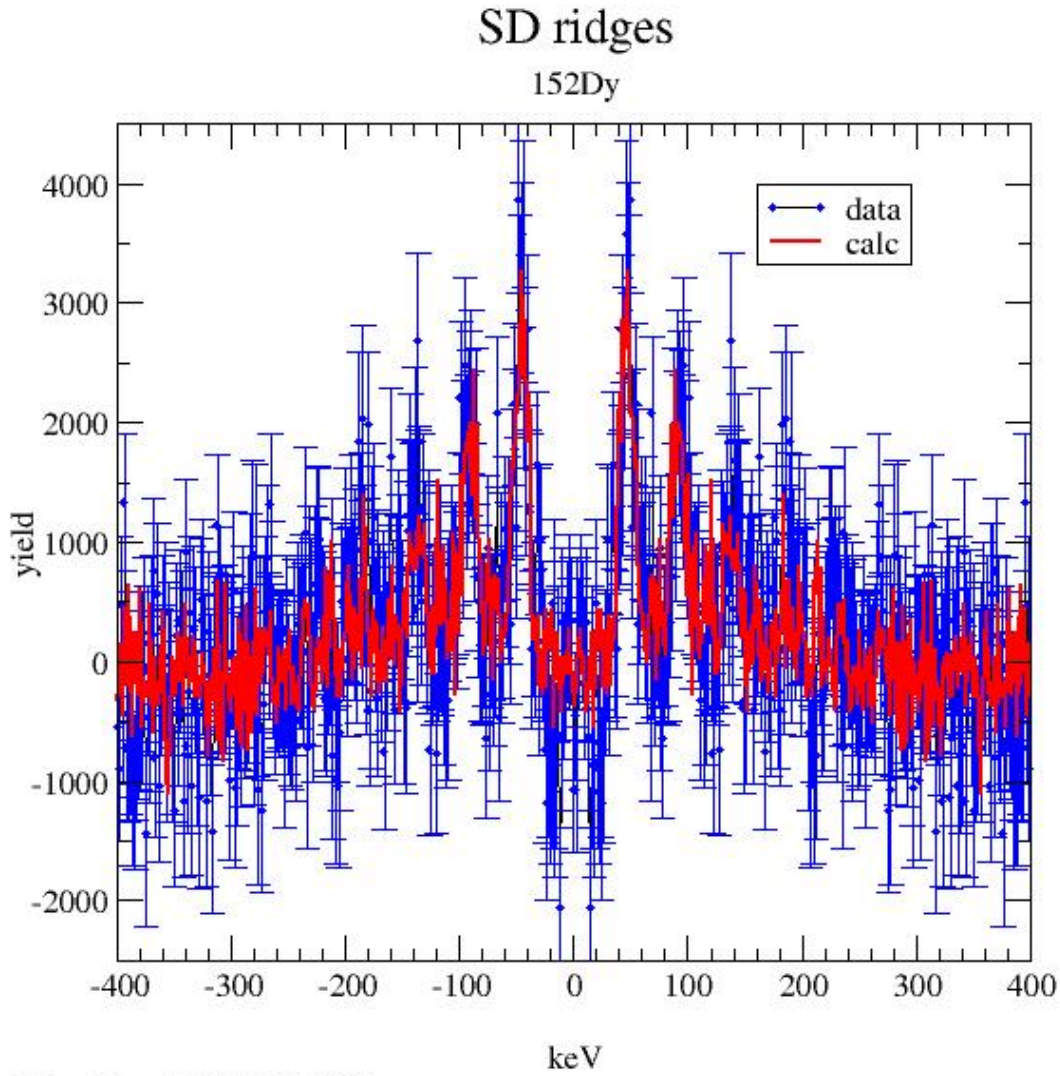


Fig. I-31. Projection of a region of a  $\gamma$ - $\gamma$  matrix normal to the diagonal in a matrix where two clean discrete SD are required. Blue is data, red is a MC calculation.

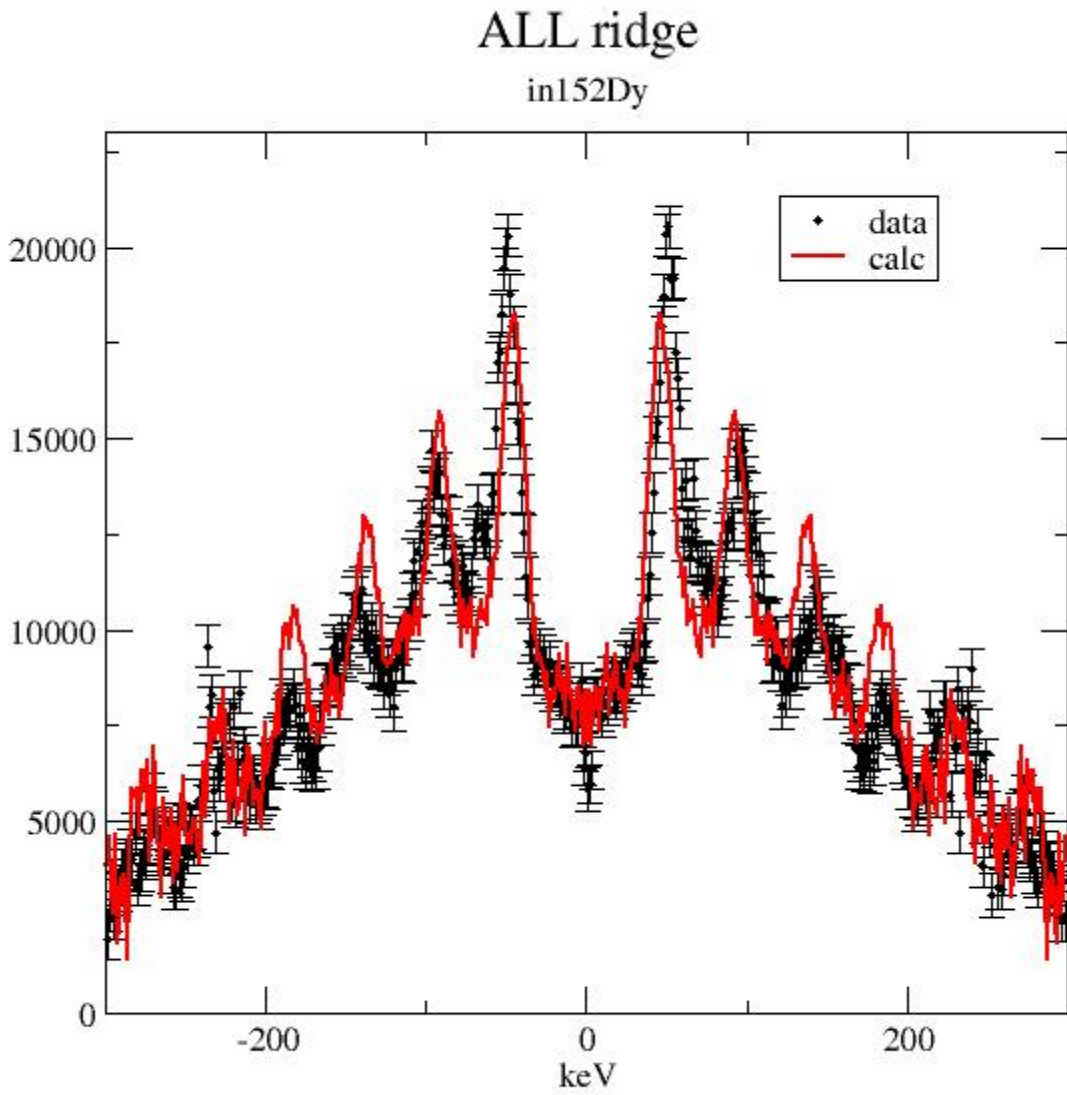


Fig. I-32. Same as Fig. I-31, but now requiring two clean ND  $\gamma$  rays before the matrix was updated. Blue is data, red is a MC calculation.

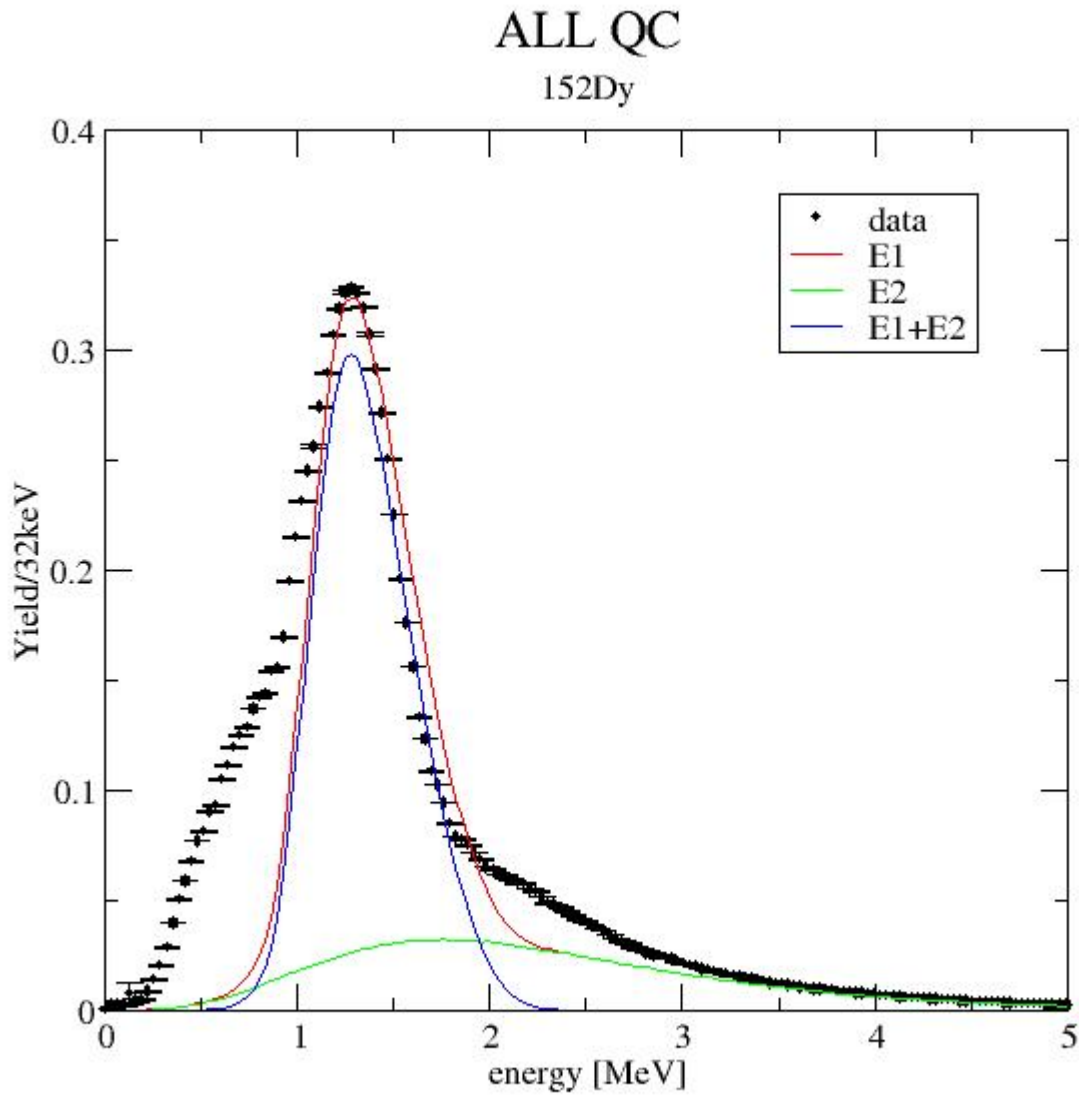


Fig. I-33. The QC of  $\gamma$  rays seen in coincidence with double gates of 1114 keV and lines just above. The normalization of this spectrum is tentative. The colored curves are the calculation of the E1 and E2  $\gamma$  rays from the *kl\_sd/kl\_a* MC code. The last step into the yrast line was not included in the MC calculation yet and will fill in the void at low energies.

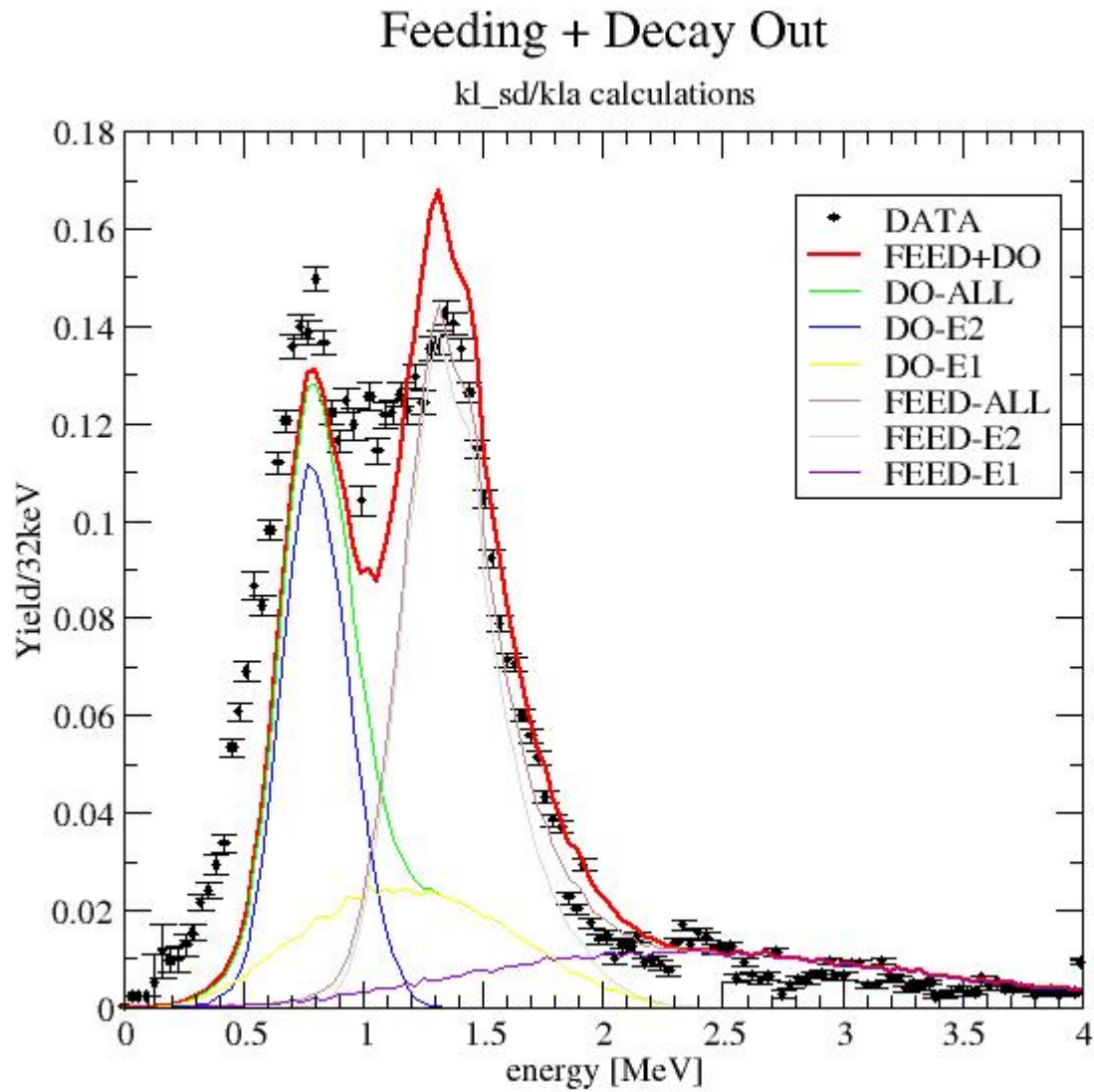


Fig. I-34. As Fig. I-33, but with double gates on clean transition in SD band 1 in  $^{152}\text{Dy}$ . There are two components, the QC from the feeding (FEED) of the SD band and the decay out (DO) of the SD band to the normal states.

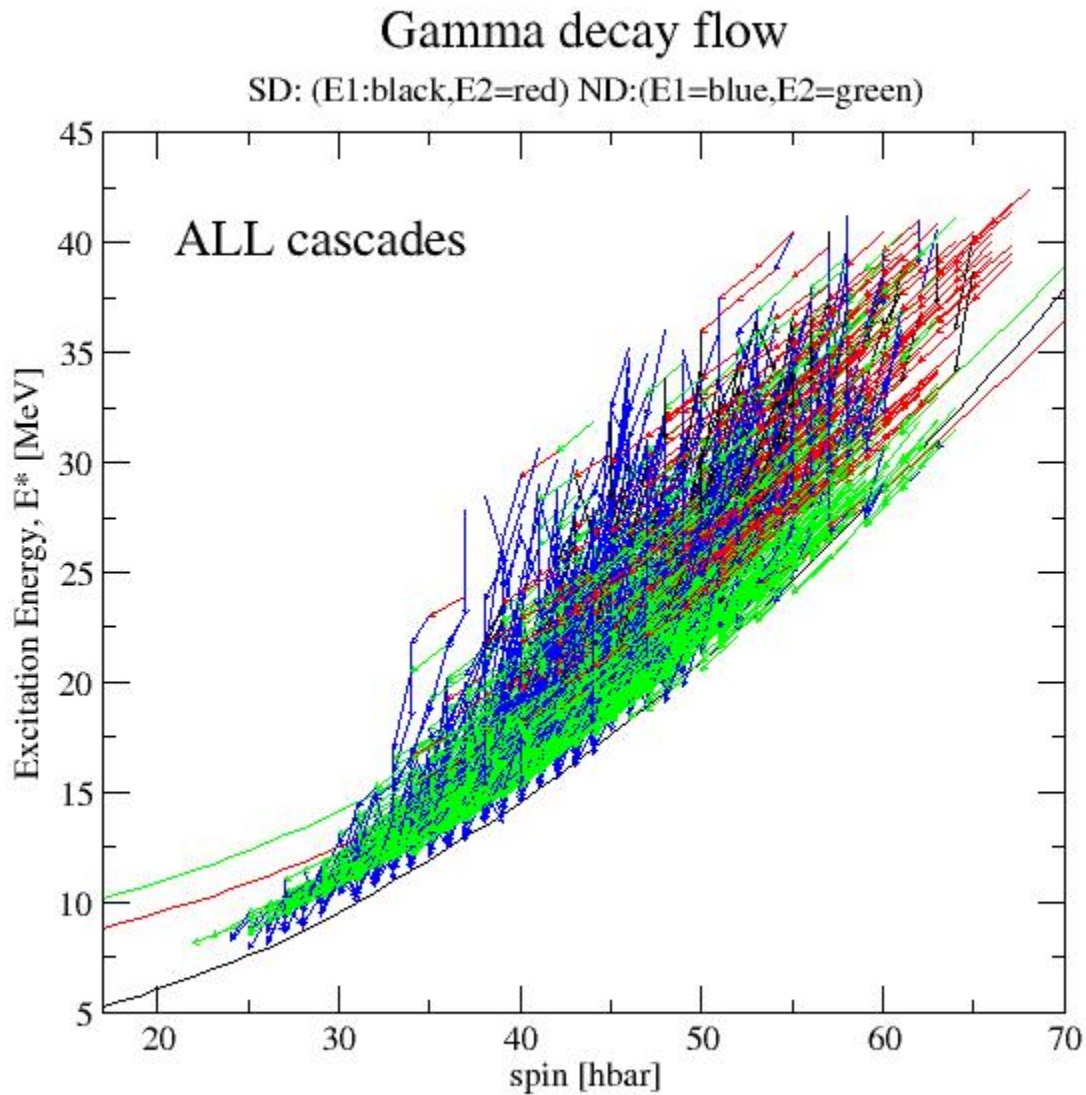


Fig. I-35. Two  $\gamma$  cascades feeding the ND states in  $^{152}\text{Dy}$ . The E1 and E2  $\gamma$  rays emitted in the SD and ND wells are shown as color-coded vectors. The solid black line is the ND yrast line and the red line is the SD yrast line. The solid green line shows the top of the barrier between the SD and ND wells.

**e.4.  $K^\pi = 4^-$  Isomers and Their Rotational Bands in  $^{168,170}\text{Er}$**  (M. P. Carpenter, R. V. F. Janssens, I. Wiedenhöver, C. Y. Wu,\* D. Cline,\* M. W. Simon,\* R. Teng,\* and K. Vetter†)

In an experiment carried out at ATLAS with Gammasphere and the CHICO array of parallel plate avalanche counters, the half-life of the known  $I, K^\pi = 4^-, 4^-$  state in  $^{170}\text{Er}$  was measured to be  $42.8 \pm 1.7$  ns. The rotational band built on this isomer was excited inelastically up to spin  $18^-$  by a  $^{238}\text{U}$  beam at  $E_{lab} = 1358$  MeV. A similar band in  $^{168}\text{Er}$  was extended to spin  $15^-$ . The wave function of the isomeric state in  $^{170}\text{Er}$  was determined from the measured  $g_K - g_R$  values, which were deduced from the intensity ratios of the  $\Delta I$

$= 1$  to  $\Delta I = 2$  transitions within the band. The dominant component consists of a two-quasiproton configuration involving the Nilsson orbits  $7/2^- [523]$  and  $1/2^+ [411]$ . In contrast, the two-quasineutron configuration involving the  $7/2^+ [633]$  and  $1/2^- [521]$  Nilsson orbits constitutes the major component for the wave function of the  $K^\pi = 4^-$  isomer in  $^{168}\text{Er}$ .

A paper reporting these results was published.<sup>1</sup>

\*University of Rochester, †Lawrence Berkeley National Laboratory.

<sup>1</sup>C. Y. Wu *et al.*, Phys. Rev. C **68**, 044305 (2003).

**e.5. Shape Coexistence and Band Crossings in  $^{174}\text{Pt}$**  (M. P. Carpenter, F. G. Kondev, R. V. F. Janssens, K. H. Abu Saleem, I. Ahmad, C. N. Davids, T. L. Khoo, A. Heinz, T. Lauritsen, J. Ressler, D. Seweryniak, I. Wiedenhöver, G. L. Poli, J. T.M. Goon,\* D. J. Hartley,\* L. L. Riedinger,\* H. Amro,† J. A. Cizewski,‡ M. Danchev,\* W. C. Ma,† W. Reviol,§ M. B. Smith,‡ and Jing-ye Zhang\*)

Collective structures in  $^{174}\text{Pt}$  were investigated by measuring in-beam  $\gamma$  rays with mass selection and the recoil-decay tagging technique. The experiment was performed with the ATLAS superconducting linear accelerator at the Argonne National Laboratory. The main emphasis of this experiment was to study high-spin states in the proton unbound systems  $^{173,175,177}\text{Au}$ , and a paper reporting the results on these nuclei was published recently.<sup>1</sup> High-spin states in  $^{174}\text{Pt}$  were populated in the  $^{92}\text{Mo}(^{84}\text{Sr}, 2p)$  and the  $^{94}\text{Mo}(^{84}\text{Sr}, 2p2n)$  reactions. Prompt  $\gamma$  rays were detected with 101 Ge detectors in the Gammasphere array. Mass and alpha decay information was obtained at the focal plane of the Fragment Mass Analyzer using the PGAC and DSSD setups.

The deduced level scheme for  $^{174}\text{Pt}$  is given in Fig. I-36. The yrast band was extended to a spin of  $(26^+)$  and a new side band established. This second band is assigned negative parity and presumed to be built on an octupole vibration at low spin. In addition, both the yrast band and octupole band are interpreted as having a weakly deformed prolate shape near their respective band heads and both bands undergo a shape change to well-deformed prolate at a rotational frequency of 0.24 MeV. At higher rotational frequencies, the sideband changes configuration from an octupole vibration to a two-quasineutron sequence and then undergoes the expected  $BC$  crossing near 0.29 MeV. A delayed  $AB$  alignment was observed for the ground-state band, which occurs at  $\hbar\omega = 0.28$  MeV. A paper reporting these results was recently published in Phys. Rev. C.<sup>2</sup>

\*University of Tennessee, †Mississippi State University, ‡Rutgers University, §Washington University.

<sup>1</sup>F. G. Kondev *et al.*, Phys. Lett. **B512**, 268 (2001).

<sup>2</sup>J. T.M. Goon *et al.*, Phys. Rev. C **70**, 014309 (2004).

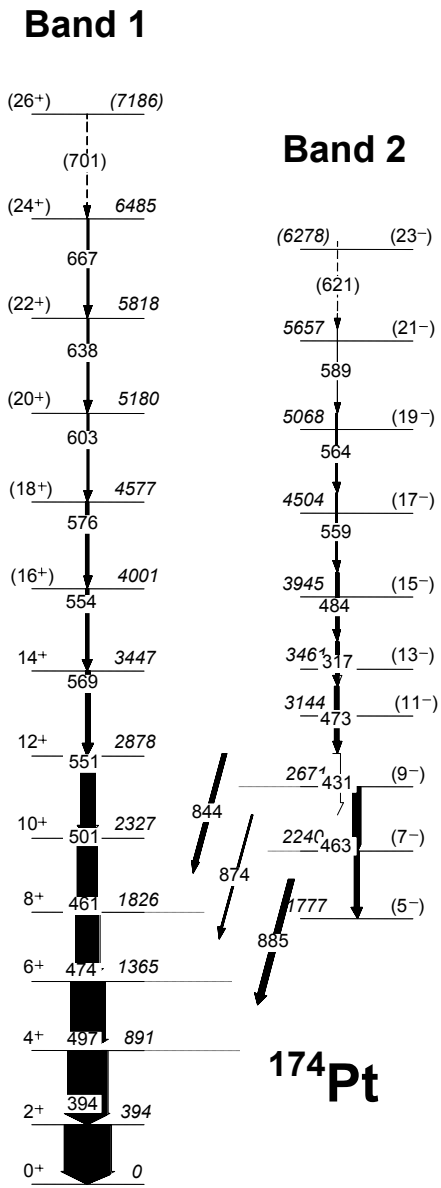


Fig. I-36 Level scheme for <sup>174</sup>Pt deduced from this work.

**e.6. Level Structure of  $^{181}\text{Tl}$**  (M. P. Carpenter, F. G. Kondev, R. V. F. Janssens, I. Ahmad, C. N. Davids, N. Hammond, T. L. Khoo, T. Lauritsen, C. J. Lister, G. Mukherjee, D. Seweryniak, S. Sinha, D. J. Jenkins,\* P. Raddon,\* R. Wadsworth,\* S. F. Freeman,† S. M. Fischer,‡ G. Jones,§ A.J. Larabee,¶ and A. Liechty¶)

With the return of Gammasphere to ATLAS, we continue our program to look at proton rich nuclei in the vicinity of the  $Z = 82$  closed proton shell. One of our most recent experiments utilized the  $^{90}\text{Zr} + ^{92}\text{Mo}$  reaction to produce  $^{181}\text{Tl}$  and  $^{181}\text{Pb}$  via the  $1p$  and  $1n$  channel, respectively. For this measurement, Gammasphere was coupled with the FMA to characterize both the ground and excited states in these two nuclei. At the focal plane of the FMA, the PGAC measured the mass, the DSSD detected the energies of both the implants and the  $\alpha$  particles emitted during the decay of the implanted ions. In addition, four Ge detectors surrounded the DSSD in order to measure  $\gamma$  rays in coincidence with detected particles.

The mid-shell Tl isotopes mimic the mid-shell Pb isotopes in that structures built on spherical, oblate and prolate shapes were established in  $^{183,185,187}\text{Tl}$ .<sup>1-3</sup> A comparison of the excitation energy of single-particle states associated with the different shapes shows that the excitation energy of the  $13/2^+$  prolate state continues to decrease as one approaches mid-shell ( $N = 102$ ) while the oblate structure built on the  $h_{9/2}$  orbital

minimizes in excitation energy at  $N = 108$  and rises in energy with decreasing neutron number. In all of these isotopes the ground state remains spherical. It is an open question whether this same trend continues beyond mid-shell.

In the analysis of our Gammasphere experiment, we followed the de-excitation of the  $i_{13/2}$  prolate band in  $^{181}\text{Tl}$  down to the 1-msec isomer built on the  $9/2^-$  oblate state. Based on our RDT measurements, most of the decay of this isomer precedes via  $\gamma$  emission to the ground state while a small  $\alpha$  decaying branch directly feeds an excited  $9/2^-$  state in the daughter nucleus,  $^{177}\text{Au}$ . Unfortunately, our measurement was not sensitive to the  $\gamma$  decay of the isomer to the spherical ground state. As a result, we only have a lower limit of 800 keV for the excitation energy of this isomer. Using this lower limit, one can say positively that both the oblate structure and the  $i_{13/2}$  prolate band rise in excitation energy when compare to the same states in  $^{183}\text{Tl}$ . In the case of the prolate structures, this is the same trend observed for the prolate bands in the even-even Pb isotones,  $^{186}\text{Pb}$  and  $^{184}\text{Pb}$ .

\*University of York, United Kingdom, †University of Manchester, United Kingdom, ‡DePaul University,

§University of Liverpool, United Kingdom, ¶Greenville College.

<sup>1</sup>W. Reviol *et al.*, Phys. Rev. C **61**, 044310 (2000).

<sup>2</sup>M. Muikku *et al.*, Phys. Rev. C **64**, 044308 (2002).

<sup>3</sup>G. J. Lane *et al.*, Nucl. Phys. **A586**, 316 (1995).

**e.7. Pair Gaps in the Normal- and Super-Deformed Wells of  $^{191}\text{Hg}$**  (P. Reiter, T. L. Khoo, T. Lauritsen, M. P. Carpenter, I. Ahmad, I. Calderin, T. Duguet, S. M. Fischer, R. V. F. Janssens, E. F. Moore, D. Nisius, S. Siem,\* P.-H. Heenen,† H. Amro,‡ T. Døssing,§ U. Garg,¶ D. Gassmann, G. Hackman, F. Hannachi,|| B. Kharraja,¶ A. Korichi,|| I.-Y. Lee,\*\* A. Lopez-Martens,|| A. O. Machiavelli,\*\* and C. Schück||)

Although about 250 superdeformed (SD) bands were found in the  $A = 150$  and  $190$  regions, the energies and quantum numbers were determined for only a handful of SD bands. The excitation energies and spins of the yrast superdeformed band in  $^{191}\text{Hg}$  were found from two single-step  $\gamma$  transitions and the quasi-continuum spectrum connecting the superdeformed and normal-deformed states. This is the first case where the energies and spins of a SD band were determined in an

odd-A nucleus. The results are compared with those from self-consistent mean-field calculations with different Skyrme interactions. The SLy4 interaction gives better agreement with experiment than other interactions, such as SkP and SkM\*.

By comparing the energies of normal-deformed (ND) and SD states in adjacent even-even and odd-A nuclei, we can extract information of the pair correlations in

the respective wells. The neutron separation energy contains information about the Fermi energy  $\lambda_N$ , the neutron pairing gap  $\Delta^{\text{pairing}}$ , as well as a so-called polarization energy  $E^{\text{pol}}$  arising from occupying a single-particle level:  $\Delta^{(2)} = (-1)^N S_n \sim \Delta^{\text{pairing}} + E^{\text{pol}} + (-1)^{N+1} \lambda_N$ . The masses of the normal- and superdeformed “ground-states” at zero rotational frequency in  $^{191,192}\text{Hg}$  give  $S_n = 9.5$  and  $8.9_{-0.3}^{+0}$  MeV, for the ND and SD wells, respectively. In other words, it is easier to remove a neutron from the SD well. With  $\lambda_N$  taken

from Hartree-Fock Boglyubov theory with the Skyrme SLy4 interaction, we obtain  $\Delta^{\text{pairing}} + E^{\text{pol}} = 1.1$  and  $1.0_{-0.3}^{+0}$  MeV for ND and SD states. ( $E^{\text{pol}}$  is expected to be around  $\pm 100$  keV.) The latter value establishes that a pair gap exists for SD states, but the uncertainties are too large to determine that its value is smaller than that for ND states.

A paper on this work was submitted to Phys. Rev. C.

\*Argonne National Laboratory and University of Oslo, Norway, †Service de Physique Nucleaire Theorique, Brussels and Oak Ridge National Laboratory, ‡Argonne National Laboratory and North Carolina State University, §The Niels Bohr Institute, Denmark, ¶University of Notre Dame, ||CSNSM, Orsay, France, \*\*Lawrence Berkeley National Laboratory.

**e.8. Narrow Spreading Widths of Excited Bands in a Superdeformed Well** (T. L. Khoo, T. Lauritsen, I. Ahmad, I. Calderin, M. P. Carpenter, G. Hackman, R. V. F. Janssens, A. Lopez-Martens,\* T. Døssing,† B. Herskind,† M. Matsuo,‡ K. Yoshida,§ F. Hannachi,\* and A. Korichi\*)

Numerous superdeformed (SD) bands were observed, which are yrast or near-yrast bands in an excited minimum of the potential energy surface. However, little is known about the excited states within the SD well. These excited states provide unusual opportunities to investigate: (i) a transition from ordered motion along the yrast line to chaotic motion above, where quantum numbers and symmetries break down, perhaps through an ergodic regime and (ii) the evolution of collectivity with increasing excitation energy, where the two-body interaction should cause the rotational strength to spread among many bands.

Data for the present work came from a Gammasphere experiment conducted at LBNL with the  $^{150}\text{Nd}(^{48}\text{Ca},4n)^{194}\text{Hg}$  reaction.  $E_\gamma - E_\gamma$  matrices were constructed from pair wise gates on SD lines, thereby selecting only transitions that survive in the SD well all the way down to the yrast SD band. Three ridges (parallel to the diagonal) with  $E_\gamma > 450$  keV can be seen (see Fig. I-37). The ridges reveal the following properties: (1) narrow spreading widths (5 - 10 keV), which increase with spin; (2) ridge spacings and, hence,  $J^{(2)}$  identical to that of SD band 1; (3) 100 - 150 participating bands (from fluctuation properties); (4) in-band probability  $\sim 1$ , for  $E_\gamma > 790$  keV; and (5) ratio of ridge intensity/total E2 strength  $\sim 1$  for  $E_\gamma < 770$  keV. The large number of unresolved bands suggests that they are excited, probably from an interval 1.5 - 2 MeV above the SD yrast line.

The properties of the 2-dimensional  $\gamma\gamma$  spectra feeding the yrast superdeformed (SD) band in  $^{194}\text{Hg}$  are unique and have never been observed in any other nuclei. In the  $\gamma\gamma$  spectra, ridges parallel to the diagonal are observed, which give rise to strong peaks in spectra that represent cuts perpendicular to the diagonal -- see Fig. I-37. Two striking properties, among many others, are observed. First, the ridges have the same separation as the discrete SD lines, i.e. the dynamical moments of inertia  $J^{(2)}$  are surprisingly the same for excited states (with 2- or more- quasiparticle excitations) as for the SD yrast (0-quasiparticle) band. Second, the ridges, which have fluctuations indicative of 100 - 150 participating excited bands, exhibit exceptionally narrow widths (5 - 10 keV) compared to those seen in normal-deformed (ND) prolate nuclei (20 - 150 keV). The narrow widths of the SD ridges indicate little fragmentation of the E2 collective flow, even though theoretical analysis by Matsuo shows that the wave functions are complicated. Nevertheless, the collective flow appears as if it originated within pure parallel bands -- with little connection between separate bands! The calculations by Matsuo also show that, for  $^{192}\text{Hg}$  (which should be very similar to  $^{194}\text{Hg}$ ), the spreading width T for collective flow is near the average spacing D between levels (for  $U = 0.7 - 1.5$  MeV); i.e. the condition for the occurrence of ergodic bands,  $T/D < 1$ , is nearly met.

An ergodic system, like a chaotic one, will explore all of the available phase space. However, unlike a chaotic

system, it does not have the extreme sensitivity on initial conditions for exponential divergence of orbits. In contrast, an ordered system “orbits” around a localized point in phase space.

The E2 flow in the excited SD bands of  $^{194}\text{Hg}$  exhibits laminar-like flow in a regime where, based on the complicated wave functions, it should be almost turbulent. Indeed, in similar bands in ND prolate nuclei, the E2 flow is much more fragmented. In other words, the SD E2 transitions manifest almost perfect

collective flow, *imitating* order, for states where the complicated wave functions should induce chaotic behavior. In this manner, they demonstrate ergodic-like behavior.

The theory of Matsuo and Yoshida shows that not all SD bands exhibit this property; only those in nuclei around  $^{192}\text{Hg}$  show this remarkable feature. A special feature in the SD well of Hg nuclei is that *high-K orbitals are prevalent* around the Fermi level.

\*CSNSM, Orsay, France, †The Niels Bohr Institute, Denmark, ‡Niigata University, Niigata, Japan, §Nara University, Nara, Japan, ¶Lawrence Berkeley National Laboratory.

<sup>1</sup>B. R. Mottelson, Nucl. Phys. **A557**, 717c (1993).

<sup>2</sup>K. Yoshida and M. Matsuo, Nucl. Phys. **A636**, 169 (1998).

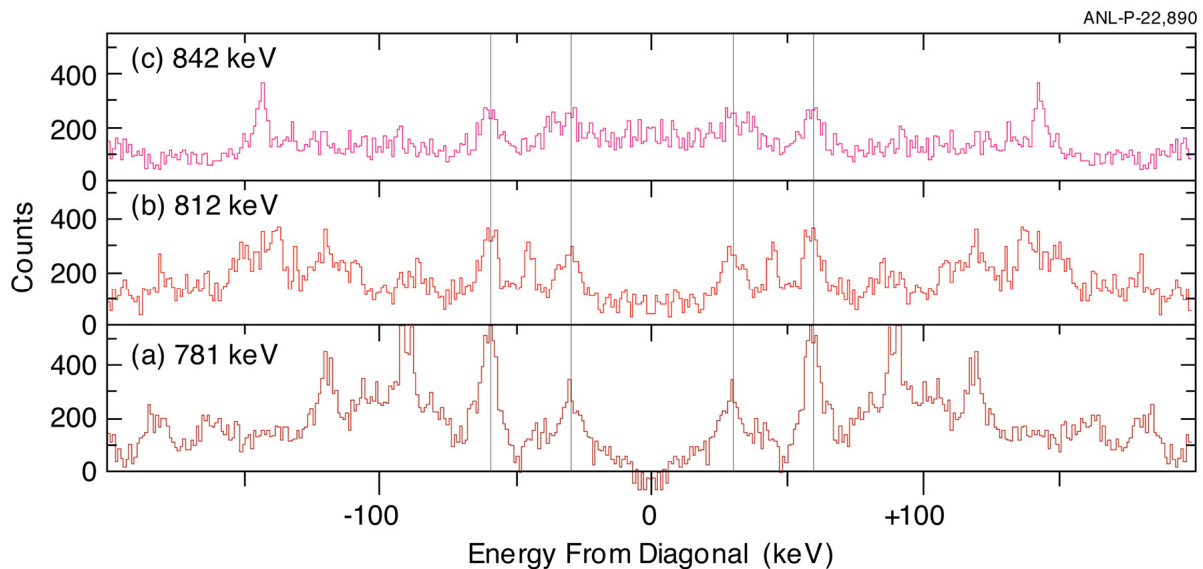


Fig. I-37. Projections perpendicular to the diagonal of an  $E_\gamma - E_\gamma$  matrix, obtained with pair wise gates on lines of the yrast superdeformed (SD) band I in  $^{194}\text{Hg}$ . The diagonal is at channel 0. The projections, which are centered at 781, 812 and 842 keV, cover 24 keV of the  $\sim 30$  keV interval between the SD lines and show peaks (marked by vertical lines) separated by about 30 keV from the diagonal. The innermost peak from the diagonal contains counts from only the quasicontinuum ridge, while the next one contains an additional contribution from a SD peak.